CASTING SIMULATION: MOLD FILLING AND SOLIDIFICATION - BENCHMARK CALCULATIONS USING *FLOW-3D*®

M. R. Barkhudarov, C. W. Hirt

Flow Science, Inc.
1325 Trinity Drive, P. O. Box 933
Los Alamos, New Mexico 87544

Abstract

Results of a numerical simulation of the filling of a sand mold with pure aluminum and its solidification are presented in this paper. The problem has been chosen as a benchmark test for the 7th International Conference on Casting Modeling and Solidification. The computations are carried out using *FLOW-3D* which is a general-purpose CFD code. The simulation involves viscous fluid flow with transient free surfaces, metal/mold heat transfer, conduction in both metal and mold, and latent heat release. The basic methods used to solve the full Navier-Stokes and energy equations, with the fluid configuration modeled by the VOF method, are presented along with the physical setup of the problem and numerical solution strategy.

M.R.BARKHUDAROV, C.W.HIRT 1 12

Introduction

The use of computer software to simulate phenomena influencing casting processes has expanded greatly in recent years. This has been driven by the inherent complexity of the processes involved, namely, interrelated fluid flow and thermal effects coupled with phase change [1,2]. Simulations provide a means of understanding the casting behavior within the mold and let designers optimize the overall process to produce the part with the desired properties at the lowest cost using available materials.

Numerical modeling of casting is a challenging task since it involves such diverse fluid flow phenomena as viscous metal flow with multiple transient free-surface boundaries, heat flow in the metal and mold, and phase change, involving different length and time scales. Generally, mold filling takes only a small fraction of the time that is needed for the casting to cool and solidify but it is considered to be important in defining the quality of the final casting [3]. Recent experimental evidence from J. Campbell [3-6] shows that the final strength of aluminum cast plates could be increased by an order of magnitude depending upon the filling behavior alone. Care must be taken to avoid splashing the metal on the sides of the mold as well as causing free surface turbulence, because these processes can introduce oxide film inclusions into the casting. These inclusions prevent the oxide coated metal from bonding with the rest of the casting. One goal of the present work is to show that such effects can be predicted given an appropriate numerical model for fluid flow and free surfaces.

The commercial, general-purpose CFD code *FLOW-3D* [7], based on a finite volume/finite difference approach, is used here to simulate the filling and solidification of a test casting. The software has unique free-surface models that accurately describe transient free surfaces with large deformations. Two methodologies, FAVOR and VOF, constitute the core of *FLOW-3D* and are described in the following sections. These methods, which are used to model geometry and free surfaces, differ from methods used in most other codes but offer many advantages.

The presented simulation was carried out as a blind test. The predicted results are to be compared with experimental data on the shape of the free surface during filling and temperature histories during solidification obtained at the University of Birmingham.

The FAVOR Method

FAVOR is an acronym for **F**ractional-**A**rea-**V**olume-**O**bstacle-**R**epresentation. It was originally developed as a means of defining obstacles of general shape within a grid composed of rectangular brick elements [8]. The concept is to define for each brick element the fractional areas of each of the six faces that are open to flow, together with the open volume of the brick. These fractions are then incorporated into the finite-volume equations of motion. For instance, convective fluxes of mass, momentum and energy between two elements at their common face must contain the open area of this face as a multiplier. If there is no open area, there can be no convective flux. The strength of the FAVOR method is the modeling flexibility it offers [9]. For heat transfer between fluids and solids, the FAVOR method gives high solution accuracy by providing a good approximation to the areas of the fluid/obstacle interface within each brick element.

M.R.BARKHUDAROV, C.W.HIRT

For an incompressible, viscous fluid, the FAVOR equations take the form:

$$\nabla \cdot (\mathbf{Au}) = 0 \tag{1}$$

$$\frac{\partial \mathbf{u}}{\partial t} + \frac{1}{V}(\mathbf{Au} \cdot \nabla)\mathbf{u} = -\frac{1}{\rho}\nabla p + \frac{1}{\rho V}(\nabla \mathbf{A}) \cdot (\mu \nabla)\mathbf{u} + g \tag{2}$$

$$\frac{\partial H}{\partial t} + \frac{1}{V}(\mathbf{Au} \cdot \nabla)H = \frac{1}{\rho V}(\nabla \mathbf{A}) \cdot (k \nabla T) \tag{3}$$

where

$$\mathbf{Au} = (A_x u_x, A_y u_y, A_z u_z), \qquad (\nabla \mathbf{A}) = (\frac{\partial}{\partial x} A_x, \frac{\partial}{\partial y} A_y, \frac{\partial}{\partial z} A_z)$$

$$H = \int C(T) dT + (1 - f_s) \cdot L$$

In these equations A_i is the open area fraction associated with the flow in the *ith* direction, V the open volume fraction, ρ density, p pressure, u_i the *ith* velocity component, μ the fluid viscosity coefficient, g gravity, H fluid enthalpy, T fluid temperature, f_s solid fraction, L latent heat, and C and k fluid specific heat and thermal conductivity coefficient, respectively. For the mold, the energy equation has the form

$$\frac{\partial T_m}{\partial t} = \frac{1}{\rho C_m V_c}(\nabla \mathbf{A}_c) \cdot (k_m \nabla T_m) \tag{4}$$

where the subscript m indicates a parameter related to the mold and the subscript c indicates quantities that are complements of the volume and area fractions. At the metal/mold interface the heat flux, q, is calculated according to

$$q = h \cdot (T - T_m) \tag{5}$$

where h is the heat transfer coefficient.

The VOF Method

The VOF, or Volume-of-Fluid, method offers a means of tracking sharp interfaces through a fixed grid of control volumes [10]. A second and very important part of the VOF method is the setting of dynamically correct interface boundary conditions. In other words, the VOF method is a numerical treatment for free surfaces or two-fluid interfaces.

The basis of VOF is the fractional volume-of-fluid, F, contained in each control volume. Control volumes can be empty, partially full or full. Partially full elements are usually those containing a free surface.

Special care must be taken to prevent smearing of the interface. This is achieved by using the donor-acceptor advection method for F as described in [10]. According to this method, the

M.R.BARKHUDAROV, C.W.HIRT

configuration of the interface in a computational element is reconstructed from the values of F in it and in surrounding cells, and then the donor- or acceptor-cell advection method is applied depending on the direction of the advection relative to the interface normal.

The equation for the F function is

$$\frac{\partial F}{\partial t} + \frac{1}{V}\nabla \cdot (\mathbf{A}\mathbf{u}F) = 0 \qquad (6)$$

The boundary conditions at the free surface are zero normal and tangential stresses.

Overview of the Solution Procedure

FLOW-3D has many options regarding numerical methods to solve equations (1)-(6). For this study we chose to use a finite volume first-order upwind differencing scheme to explicitly discretize advection terms in the Navier-Stokes equations, Eq. (2), in three dimensions using a non-uniform staggered grid of rectangular cells. Viscous terms were represented explicitly using a centered differencing technique. Due to the incompressibility of the fluid, the pressure and velocities in the continuity equation, Eq. (1), have to be approximated implicitly at each time step. The resulting linear algebraic equations for pressure and velocity were solved iteratively using the successive overrelaxation (Gauss-Seidel, or SOR) method [11]. A detailed description of the numerical algorithm can be found elsewhere [*e.g.* 10].

Overview of the Modeling Strategy and Results

Geometry and Mesh Setup

Figure 1 shows the geometry and dimensions of the casting. The mesh setup and the numerical representation of the geometry are given in Figure 2. The number of cells in the mold/cavity

domain, excluding fictitious cells at the six domain boundaries which are introduced to enforce the boundary conditions, is 58905, with the smallest cell size of 2.5 *mm* across the sprue and the plate thickness.

The properties of the metal and sand mold used in the calculation, are given in Tables 1 and 2 (data compiled from literature was specifically provided for the benchmark test, except for the heat transfer coefficient which was chosen by the authors).

Table 1. Aluminum and Sand Properties

	solid metal	liquid metal	sand mold
density, kg/m^3	2570	2400	1520
thermal conduct., *W/m/C*	220	110	0.65
specific heat, *J/kg/C*	1100	1100	987
viscosity, *kg/m/s*	-	0.02	-
heat transfer coeff., $W/m^2/C$			1500

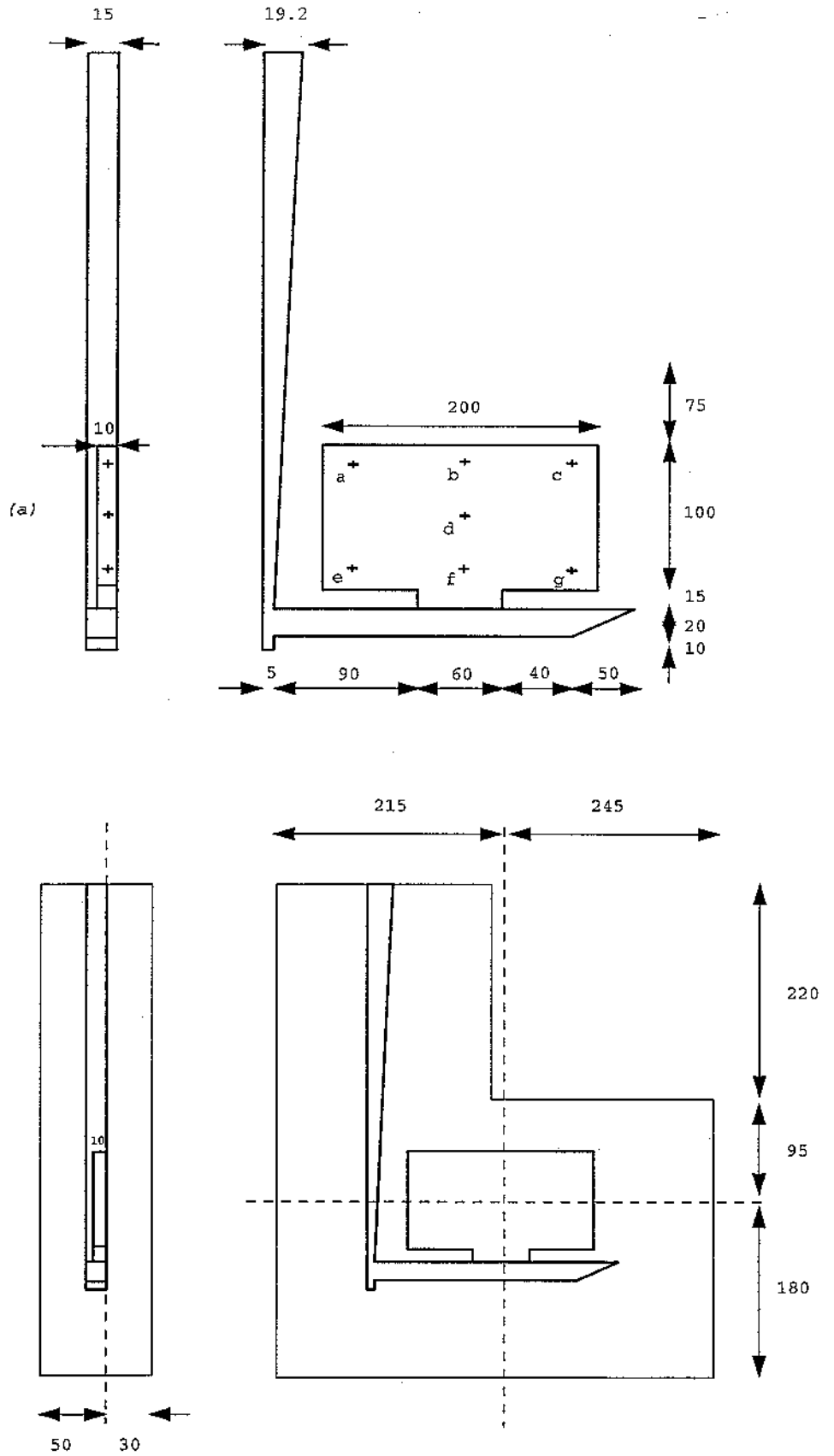

Figure 1. Geometry and dimensions of the test casting and thermocouple *a-g* locations, marked by crosses.

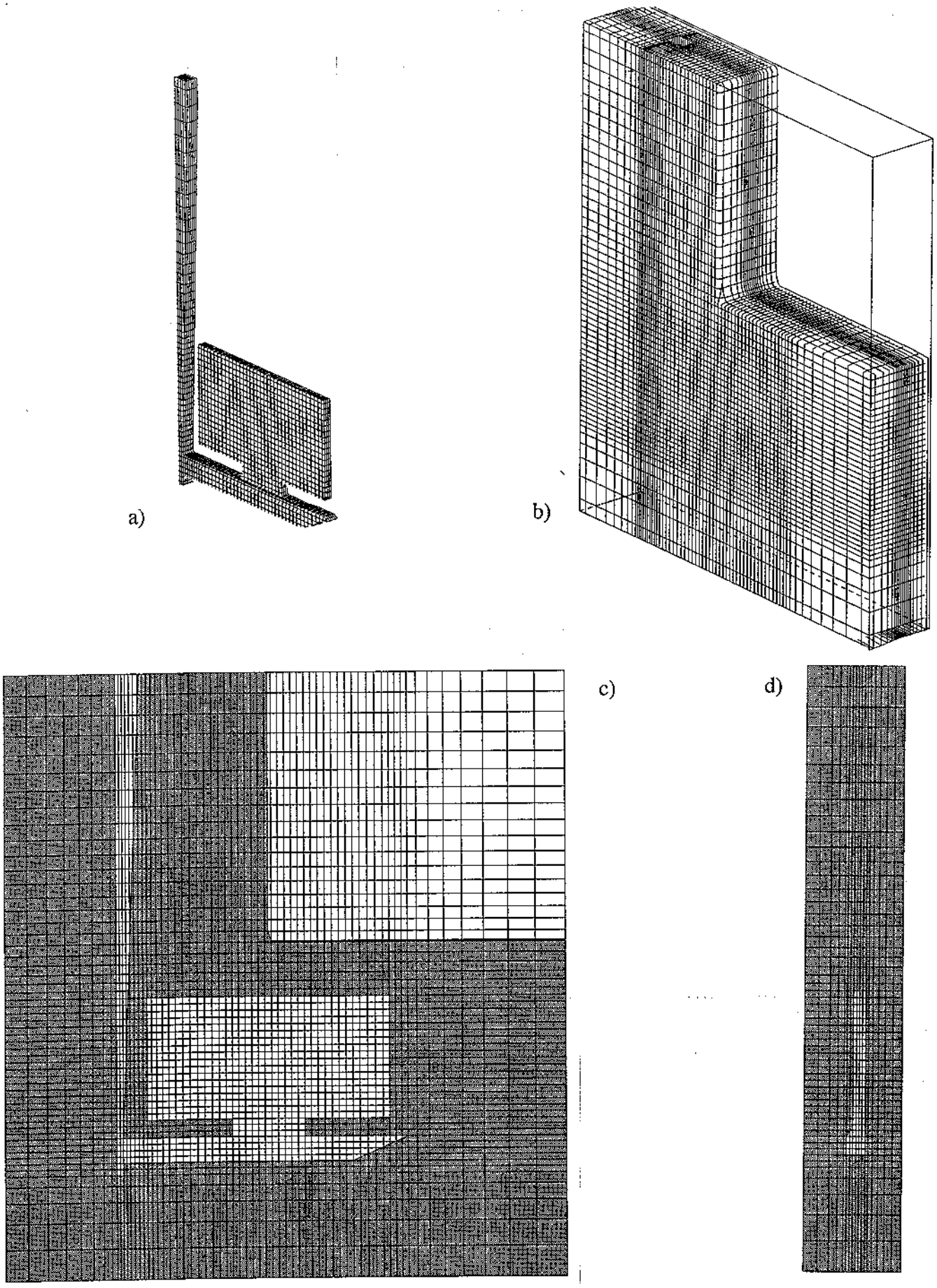

Figure 2. Numerical mesh and geometry setup: (a) the mold cavity and runner, (b) the outside mold surface, (c) x-z and (d) y-z mesh and geometry setup.

Table 2. Latent Heat Release in Aluminum

Temperature, C	$-L\frac{df_s}{dT}$, $J/kg/C$
below 635	0
635 (solidus)	7700
640	13550
645	11000
650	11500
659	17530
above 660.4 (liquidus)	0

Initial and Boundary Conditions

The pouring basin is not included in the calculation. Instead, a stagnation pressure boundary condition is used at the sprue entrance to simulate the constant level of metal which during the experiment was kept at 40 *mm* above the sprue. The value of the pressure at the boundary is 1000 Pa (assuming the ambient, or void, pressure is zero). The term *stagnation* means that the metal enters the sprue from rest, assuming that metal velocities in the pouring basin are much lower than those in the sprue. The temperature of the incoming metal is equal to 700°C. The outside boundaries of the mold are set at a room temperature of 25°C.

Initially, the mold cavity is empty and the mold is at 25°C. The flow is initiated at time t=0.0 *s* by the applied boundary pressures and corresponds to an experiment in which the stopper is removed from the pouring basin instantaneously without disturbing the metal in it.

Filling Stage Simulation

The predicted filling time is 1.83 seconds. Figures 3 and 4 show snapshots of the filling sequence at eight times: 0.24, 0.5, 0.74, 1.0, 1.24, 1.5, 1.74 and 2.0 seconds. The snapshots represent the two-dimensional shape of the free surface in the center plane of the plate. The sprue is only shown at 0.24 *s* since it is completely full on all other plots. Temperature distribution at the end of the filling is also shown in Figure 4d.

The viscosity coefficient used here is five times larger than the molecular viscosity of pure aluminum. The larger viscosity corresponds to a Reynolds number of 1600 in the sprue. The larger value of μ was used to increase the filling time, which still differs from the experimental value of 2.2 *s* by 17%, while the actual molecular value gave a filling time of 1.5 *s*. The filling time is mainly defined by the friction between the mold and the metal occurring in the narrowest part of the sprue where the flow is the fastest (about 2.5 *m/s*). Further increase of μ appeared to significantly affect the flow in the plate cavity.

Although *FLOW-3D* can treat the effects of surface tension, they are not taken into account in this study due to large values of Weber and Bond numbers during filling:

$$We = \frac{\rho d U^2}{\sigma} > 60, \qquad Bo = \frac{g\rho d^2}{\sigma} > 15$$

where d is the half width of the ingate (30 *mm*), U is the characteristic velocity (1 *m/s*) and σ is the surface tension coefficient (1.2 *N/m*). Flow of air in the void region also was not included in

M.R.BARKHUDAROV, C.W.HIRT

the simulation. We assumed the air escaped through the porous sand mold and its pressure remained constant.

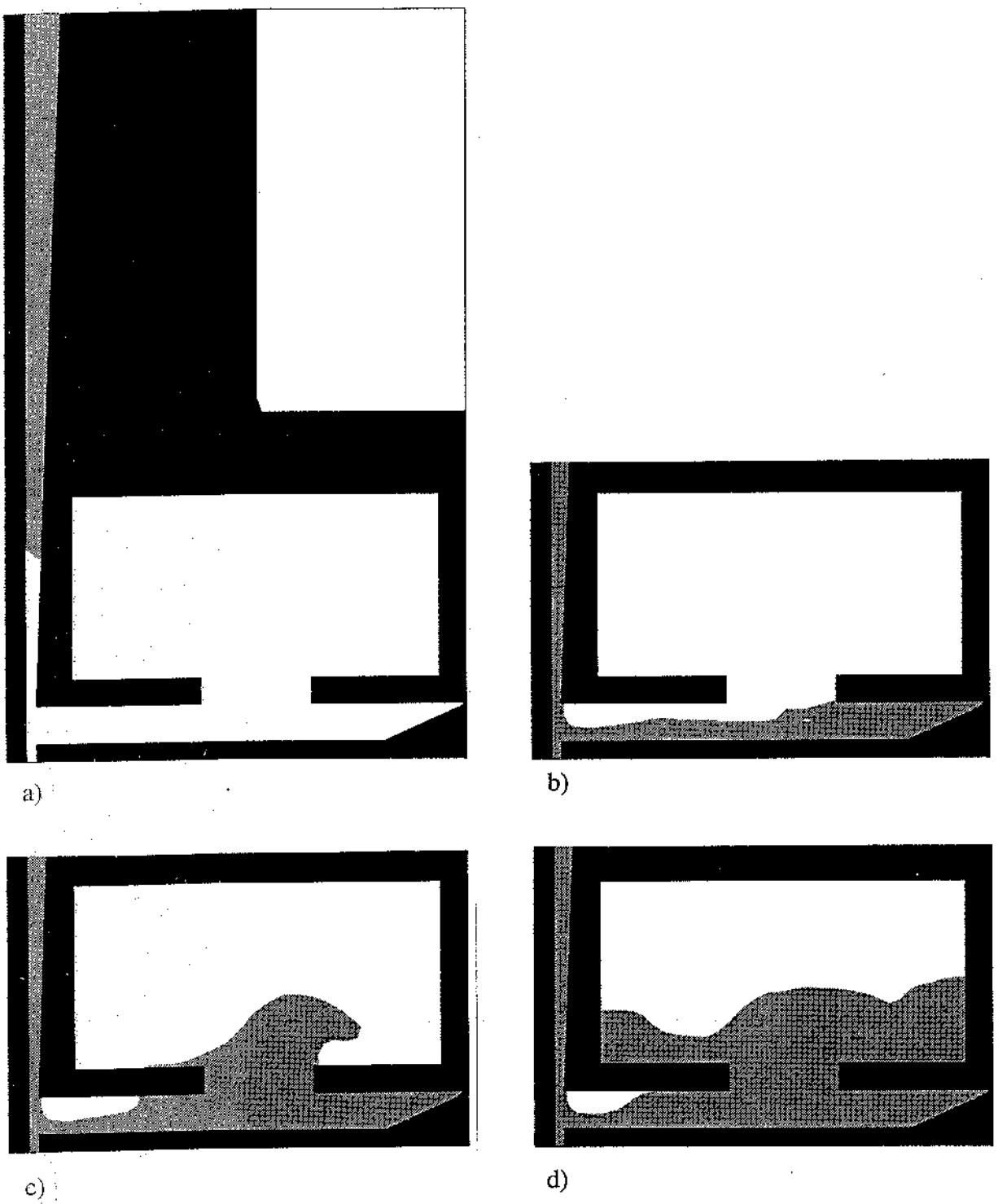

Figure 3. Views of the fluid configuration plotted in the plate symmetry plane at: (a) t=0.24 *s*, (b) t=0.5 *s*, (c) t=0.74 *s* and (d) t=1.0 *s*. The sprue is completely full in plots (b)-(d).

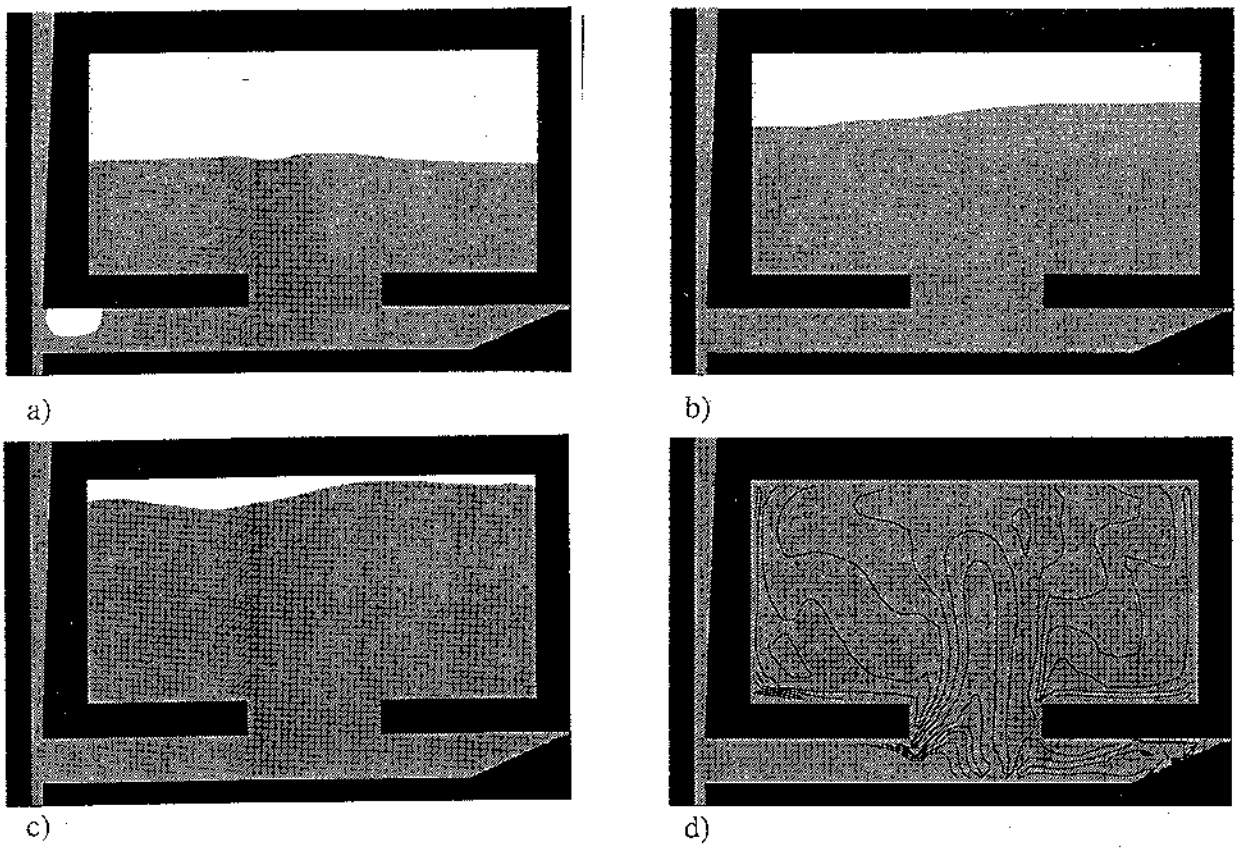

Figure 4. Same as in Figure 3 at: (a) t=1.24 *s*, (b) t=1.5 *s*, (c) t=1.74 *s* and (d) t=2.0 *s*. Lines denote isotherms at t=2.0 *s* with the minimum and maximum temperatures in the plate 653 and 663 degrees Celsius, respectively.

Solidification Stage Simulation

The simulation of cooling and solidification of the metal was carried out as a continuation of the filling process from the time the filling simulation finished. Fluid flow calculations were not included at this stage since thermal conduction prevails in redistributing the metal energy. The energy equation was solved both in the metal and mold using a fully implicit algorithm. An enthalpy approach was used to describe the release of the latent heat, where the enthalpy in the freezing range was specified as a function of temperature using data from Table 2. The simulation was carried out to 250.0 seconds measured from the start of the filling. Figures 5 and 6 show the calculated temperatures at the seven thermocouple locations in the plate indicated in Figure 1. The variation of temperature at the thermocouple locations during filling was not significant as can be seen in Figure 6d, where temperature at thermocouple *f* (nearest to the gate) is shown. The predicted total solidification time is 35 seconds.

Simulation Diagnostics

Table 3 summarizes some of the diagnostics related to the simulation, including an approximate setup time, CPU time, *etc.* All calculations were performed using an HP Apollo Model 715/50 workstation with 64 Mb of memory.

Table 3. Simulation Diagnostics (total number of cells 71630).

	setup time, *hrs*	Run time, *s*	Average time step, *s*	CPU time, *s*
Filling	2	1.83	0.0007	50500
Solidification	0.1	250	0.12	43000

M.R.BARKHUDAROV, C.W.HIRT

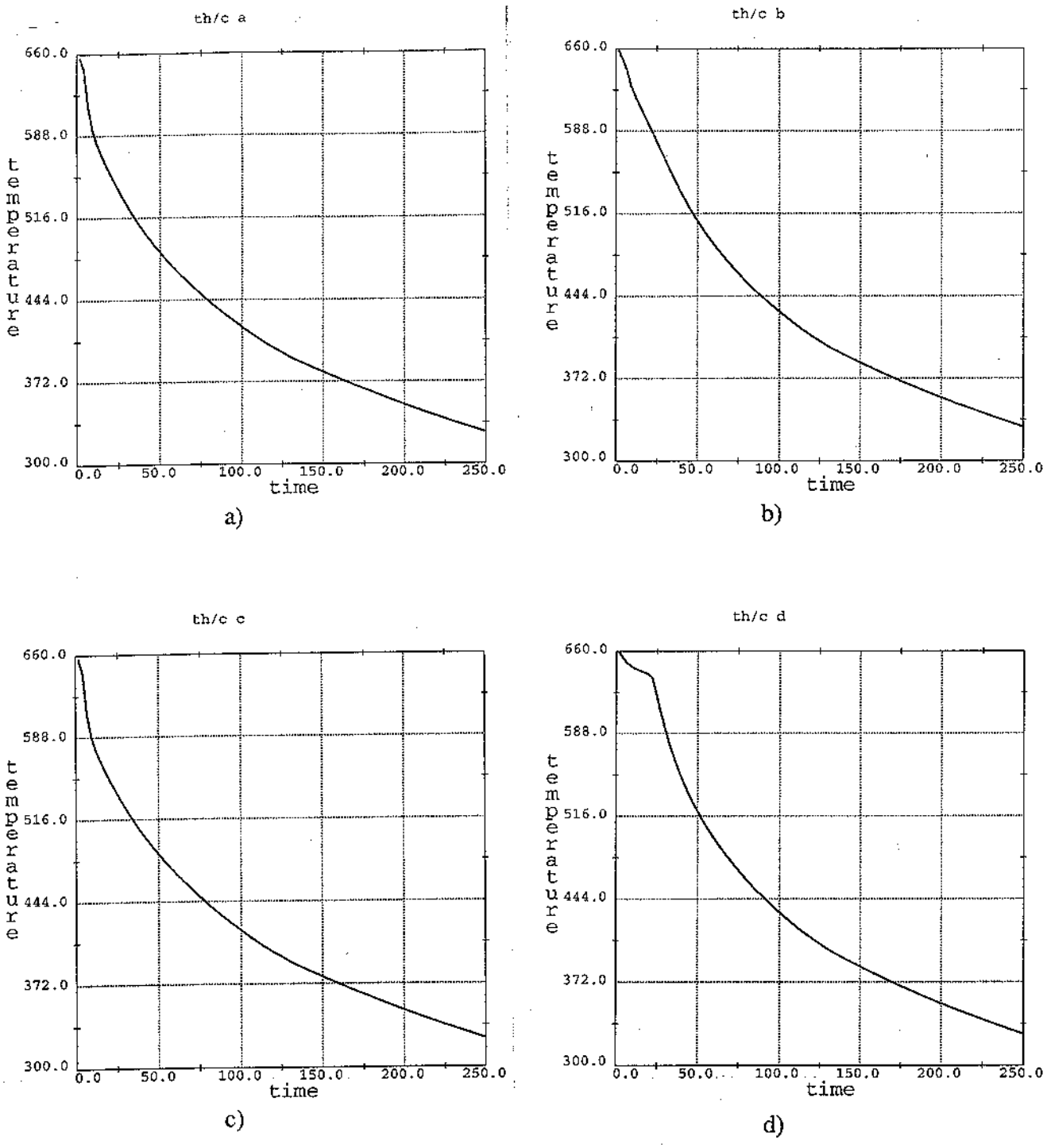

Figure 5. Predicted temperatures at locations (a) *a*, (b) *b*, (c) *c* and (d) *d* shown in Figure 1.

M.R.BARKHUDAROV, C.W.HIRT

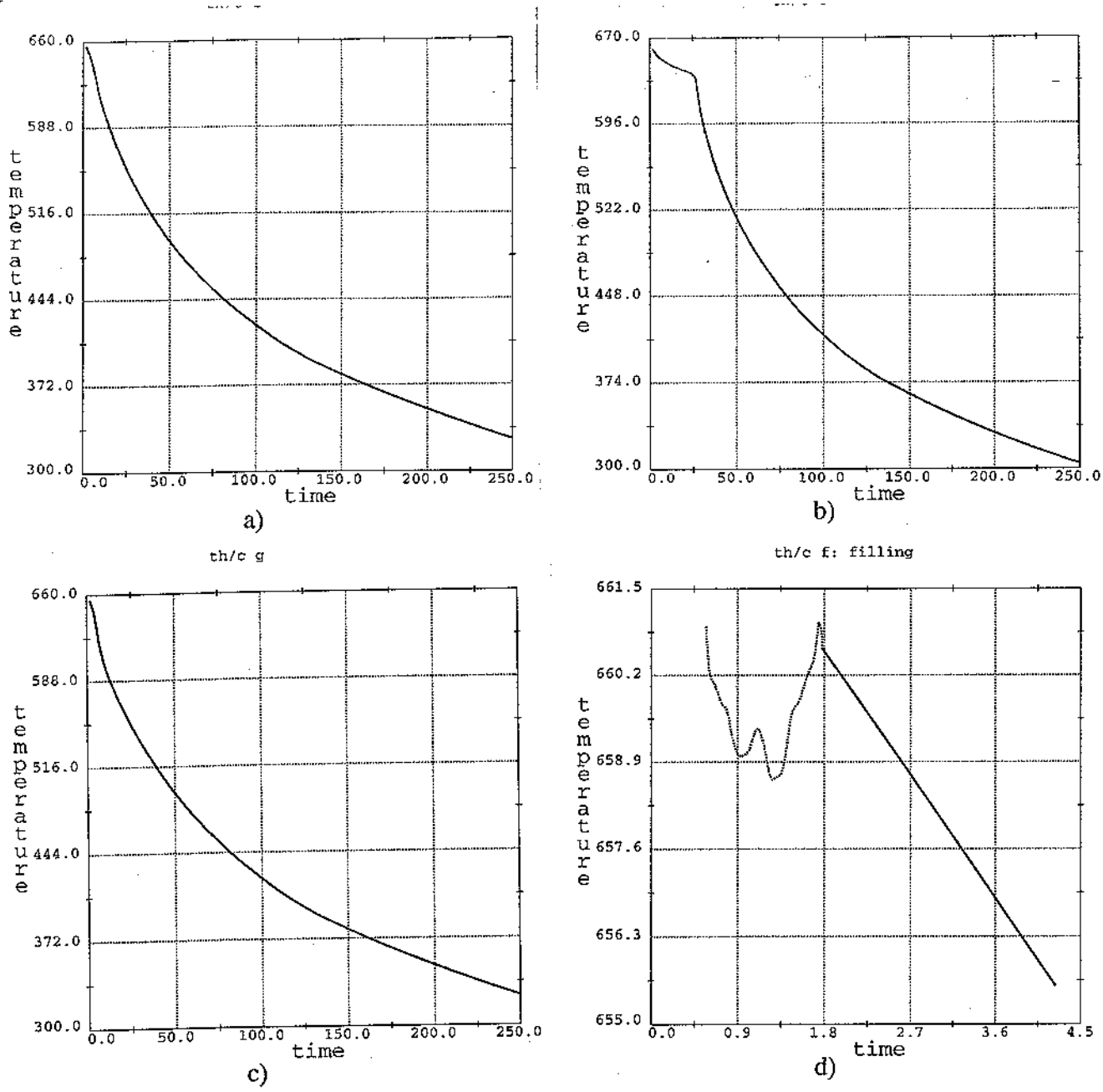

Figure 6. Predicted temperatures at locations (a) *e*, (b) *f* and (c) *g*. Temperature variation during filling (dotted line) at location *f* is shown in (d) on a magnified scale.

References

1. A. Cottrel, An Introduction to Metallurgy (London, Edward Arnold Publishers, 1975), 23-41.

2. M. C. Flemings, Solidification Processing (New-York, McGraw-Hill Book Co., 1974), 341-352.

3. J. Campbell, Castings (London, Butterworth Heinmann, 1991), 27-85.

4. J. Campbell, "Thin Wall Castings," Materials Science and Technology, 4 (1988), 194-214.

5. J. Campbell, "Invisible Macrodefects in Castings", Journal de Physique IV, 3 (1993), 861-872.

6. N. R. Green and J. Campbell, "Statistical Distributions of Fracture Strengths of Cast Al-7Si-Mg Alloy", Materials Science and Engineering, A173 (1993), 261-266.

7. J. M. Sicilian, C. W. Hirt, and R. P. Harper, "FLOW-3D: Computational Modeling Power for Scientists and Engineers", (Report FSI-87-00-01, Flow Science, Inc., 1987).

8. C. W. Hirt and J. M. Sicilian, "A Porosity Technique for the Definition of Obstacles in Rectangular Cell Meshes", (Paper presented at the 4th International Conference on Ship Hydrodynamics, Washington D.C., September 1985).

9. C. W. Hirt, "Volume-Fraction Techniques: Powerful Tools for Wind Engineering", Journal of Wind Engineering and Industrial Aerodynamics, 46 & 47, (1993), 327-338.

10. C. W. Hirt and B. D. Nichols, "Volume of Fluid (VOF) Method for the Dynamics of Free Boundaries", J. Comput. Phys., 39, (1981), 201-225.

11. J. M. Ortega and W. C. Rheinboldt, Iterative Solution for Nonlinear Equations in Several Variables, (New York, Academic Press, 1970).

12